The Meteoritical Society

*Meteoritics & Planetary Science* 46, Nr 5, 681–689 (2011)
doi: 10.1111/j.1945-5100.2011.01182.x

# Rb-Sr and Sm-Nd isotopic systematics of the lherzolitic shergottite GRV 99027

Tao LIU[1,2,3], Chaofeng LI[1,3], and Yangting LIN[1*]

[1]Key Laboratory of the Earth's Deep Interior, Institute of Geology and Geophysics, Chinese Academy of Sciences, Beijing 100029, China
[2]Guangzhou Institute of Geochemistry, Chinese Academy of Sciences, Guangzhou 510640, China
[3]Graduate School of Chinese Academy of Sciences, Beijing 100039, China
[*]Corresponding author. E-mail: LinYT@mail.igcas.ac.cn

*(Received 02 May 2010; revision accepted 16 January 2011)*

**Abstract**–Rb-Sr and Sm-Nd isotopic analyses of the lherzolitic shergottite Grove Mountains (GRV) 99027 are reported. GRV 99027 yields a Rb-Sr mineral isochron age of 177 ± 5 (2σ) Ma and an initial $^{87}Sr/^{86}Sr$ ratio ($I_{Sr}$) of 0.710364 ± 11 (2σ). Due to larger uncertainties of the Sm-Nd isotopic data, no Sm-Nd isochron age was obtained for GRV 99027. The $\varepsilon^{143}Nd$ value is estimated approximately +12.2, assuming an age of 177 Ma. The $I_{Sr}$ of GRV 99027 is distinguishable from other lherzolitic shergottites, confirming our previous conclusion that it is not paired with them (Lin et al. 2005). The new data of GRV 99027 support the same age of approximately 180 Ma for most lherzolitic shergottites, and fill the small gap of $I_{Sr}$ between Allan Hills A77005 and Lewis Cliff 88516 (Borg et al. 2002). All available data are consistent with a single igneous source for the intermediate subgroup of lherzolitic shergottites.

## INTRODUCTION

Shergottites are a common group of Martian meteorites (51 out of 63 samples), and they are classified into three petrographic types: basaltic, olivine-phyric, and lherzolitic (or peridotitic) (McSween 1994; Goodrich 2002). In addition, based on their geochemistry, shergottites can also be divided into light rare earth element (LREE)-depleted, intermediate, and LREE-enriched subgroups (Symes et al. 2008). A remarkable feature of shergottites is their young mineral isochron ages (165–475 Ma) in comparison with other Martian meteorites (≥1300 Ma) (Nyquist et al. 2001). This is inconsistent with the prevailing "old" Martian surface as indicated by the high density of craters. The debate on crystallization ages of shergottites is a long-standing controversial issue and was reinvigorated by reports of Pb-Pb whole rock isochron ages of ≥4.0 Ga (Bouvier et al. 2005a, 2008, 2009) and in situ U-Pb analyses of baddeleyite (Herd et al. 2007; Misawa and Yamaguchi 2007; Ozawa et al. 2009). These "old" Pb-Pb ages were interpreted as time of crystallization, whereas the "young" radiometric mineral isochrons were reset either by alteration (Bouvier et al. 2005b) and/or severe impact events (Bouvier et al. 2008).

As a small subgroup, lherzolitic shergottites, have only 12 meteorites reported. Except for the newly found Grove Mountains (GRV) 020090 and Roberts Massif (RBT) 04262/04261, both of which are enriched in LREE and other incompatible elements (Miao et al. 2004; Anand et al. 2008.; Lin et al. 2008a; Usui et al. 2008), most lherzolitic shergottites belong to the intermediate subgroup and share similar petrological and mineralogical features (e.g., McSween 1994; Bridges and Warren 2006). Furthermore, only five of them (Allan Hills [ALH]A77005, Lewis Cliff [LEW] 88516, Yamato [Y-]-793605, Y-000097, and Y-984028) have been studied for Rb-Sr and/or Sm-Nd isotopes, reporting same mineral isochron ages of approximately 180 Ma with similar initial $^{87}Sr/^{86}Sr$ ratios and $\varepsilon^{143}Nd$ values except for small differences in the initial ratios between ALHA77005 and LEW 88516 (Shih et al. 1982, 2011; Jagoutz 1989; Morikawa et al. 2001; Borg et al. 2002; Misawa et al. 2006, 2008). These meteorites were probably launched from the same igneous unit on Mars by a single impact event, or ejected from different but similar sites by several events. In the case of the latter, their similarities in petrography and geochemistry have important constraints on the magmatic evolution of

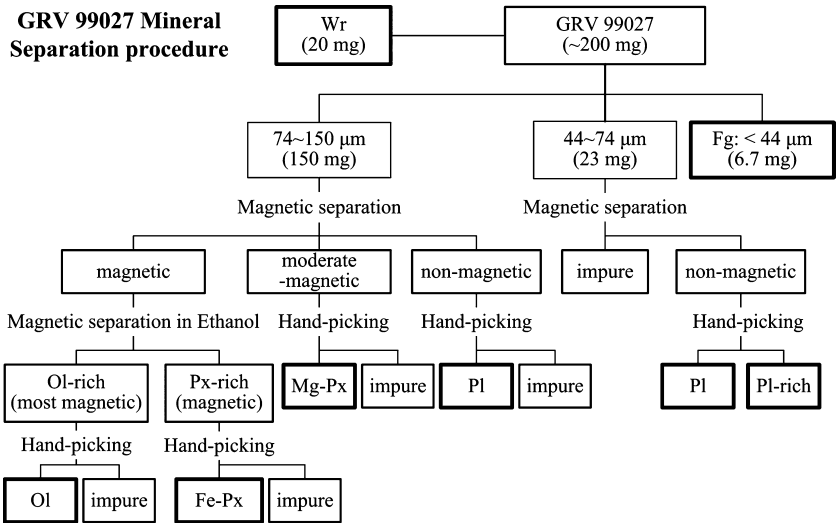


Fig. 1. Flowchart of mineral separation procedure. Each mineral separate was further purified (>99%) by hand-picking. Bold lined boxes are the analyzed samples. All mineral fractions were leached with 0.5 M HCl before digestion. Wr, whole rock; Fg, fine-grained fraction; Px, pyroxene; Ol, olivine; Pl, plagioclase.

Mars. It is obvious that dating on new meteorites is a key point to clarify the radiometric ages of lherzolitic shergottites.

GRV 99027 was found in Grove Mountains, Antarctica, and was classified as the fourth lherzolitic shergottite (Lin et al. 2002, 2003). It is nearly identical to other lherzolitic shergottites of the intermediate subgroup in petrography, mineral chemistry, and bulk composition (Hsu et al. 2004; Lin et al. 2005, 2008b), and has the same ejection age of approximately 4 Ma (Kong et al. 2007). This suggests that GRV 99027 may have been ejected from the same igneous unit on Mars as the others, by a single impact event (Lin et al. 2005, 2008b; Kong et al. 2007). In this work, we have conducted Rb-Sr and Sm-Nd isotopic analyses on GRV 99027 to determine its crystallization age and initial Sr and Nd isotopic compositions. The new data will have key constraints on the genetic relationship of GRV 99027 to other lherzolitic shergottites, hence clarify if they originated from the same igneous unit on Mars.

## PETROLOGY OF GRV 99027

GRV 99027 weighs 9.97 g and comprises two textural regions: poikilitic and interstitial (Lin et al. 2002). The poikilitic region consists of low-Ca pyroxene oikocrysts and olivine chadacrysts both with minor inclusions of euhedral chromite. The interstitial region consists mainly of subhedral or euhedral low-Ca pyroxene, augite and olivine with interstitial plagioclase and minor chromite, ilmenite, merrillite, and apatite (Lin et al. 2005). The REE and other trace element concentrations of the constituent minerals of GRV 99027 were analyzed in situ with secondary iron mass spectrometry (SIMS) by Hsu et al. (2004) and Lin et al. (2005), and are similar to those of other lherzolitic shergottites. The bulk composition of GRV 99027 is moderately LREE-depleted, but with distinctly lower absolute bulk concentrations of REEs than other members of the same subgroup (Lin et al. 2008b), probably due to a lower abundance of phosphates (Lin et al. 2008b). GRV 99027 experienced intensive shock metamorphism followed by a high degree of thermal metamorphism, as indicated by the existence of recrystallized plagioclase and the homogeneity of individual grains of olivine and pyroxenes (Lin et al. 2005; Wang and Chen 2006).

## ANALYTICAL TECHNIQUES

The samples of GRV 99027 studied in this work are aliquots of the same sample analyzed for the bulk composition in our previous study (Lin et al. 2008b). About 200 mg of a fusion-free sample of GRV 99027 was used in this study, including 20 mg of the bulk sample (< 74 μm, labeled Wr), 150 mg of a coarse-grained fraction (149–74 μm), 23.1 mg of a medium-grained fraction (74–44 μm), and 6.7 mg of a fine-grained fraction (< 44 μm, labeled Fg). Both the coarse- and middle-size fractions were used for mineral separation. The sample allocation and mineral separation flow chart are shown in Fig. 1. The coarse-grained part was first separated into nonmagnetic, moderately magnetic, and magnetic fractions using hand magnets with different magnetic intensities. The magnetic sample was further separated into an olivine-rich fraction and a pyroxene-rich

fraction (labeled Fe-Px) in analytical grade of ethanol in a glass beaker using a hand magnet. The moderately magnetic fraction mainly contains Mg-rich pyroxene (labeled Mg-Px) and the nonmagnetic fraction is dominated by plagioclase. Each mineral separation was further purified (≥99%) by hand-picking under stereo microscope. After hand-picking, the remainders of the coarse-grained fractions were combined and used as an individual sample (labeled impure), while the remainder of the middle-grained nonmagnetic fraction after hand-picking plagioclase served as another fraction (labeled Pl-rich).

Chemical procedures were carried out in the ultraclean room of the Laboratory for Radiogenic Isotope Geochemistry, the Institute of Geology and Geophysics, Chinese Academy of Sciences (CAS). Water was deionized using a Milli-Q Element system (Millipore, resistance >18.2 MΩ). All acids were purified twice by subboiling distillation in PTFE distillers.

All mineral fractions (Pl, Mg-Px, Fe-Px, and Ol [divided into two samples: Ol-1, Ol-2]), Pl-rich and impure mineral (labeled Rej) fractions were cleaned first in Milli-Q water with ultrasonic, and then washed with 0.5 M HCl for 10 min at room temperature to remove possible contamination. One unleached (only cleaned in Milli-Q water) whole rock sample (Wr1) was also analyzed. Another aliquot of the whole rock and the fine-grained fraction were leached in 0.5 M HCl for 10 min at room temperature, and the residues were labeled Wr2-R, Fg-R, respectively. The combined mineral acid leachates (labeled ΣMin-L), whole rock acid leachate (labeled Wr2-L), and fine-grained acid leachate (labeled Fg-L) were also analyzed as individual sample solutions.

The powdered samples were digested in a mixed acid of concentrated 80 μL HF + 30 μL $HNO_3$ + 5 μL $HClO_4$ in 2.5 mL Teflon-PFA screw-cap vessels and spiked with appropriate amounts of mixed $^{87}$Rb-$^{84}$Sr and $^{149}$Sm-$^{150}$Nd tracer solutions. The sealed vessels were heated at 120 °C on a hotplate for 48 h and vibrated once every 4 h in daytime. After that, the sample solutions were evaporated at 90 °C to remove $SiF_4$. Concentrated 80 μL HF + 30 μL $HNO_3$ was added to the residues, then the sealed vessels were heated again on the hotplate at 120 °C for an additional 5 days. After complete digestion, the solutions were evaporated to dryness at 180 °C. The residues were redissolved with 150 μL of 6 M HCl, and heated on the hotplate overnight. The solutions were again evaporated at 120 °C. Finally, the sample residues were redissolved with 70 μL of 3.5 M $HNO_3$ and kept on the hotplate at 70 °C ready for column chemistry. The leachates (ΣMin-L, Wr2-L, Fg-L) were evaporated at 120 °C, redissolved with 70 μL of 3.5 M $HNO_3$, and appropriate amounts of the mixed $^{87}$Rb-$^{84}$Sr and $^{149}$Sm-$^{150}$Nd tracer solutions were added.

The separation procedure for Rb-Sr and Sm-Nd consists of three processes. First, Sr was separated from Rb using a Teflon minicolumn (30 mm long × 1 mm i.d.) filled with about 30 μL Sr-spec® resin (50–100 μm) as described by Misawa et al. (2000) and Li et al. (2005). The sample solution of 70 μL of 3.5 M $HNO_3$ was loaded onto the column. Rubidium and the REEs were eluted with 40 μL of 3.5 M $HNO_3$. After rinsing with 0.4 mL of 3.5 M $HNO_3$, Sr was stripped using 0.18 mL Milli-Q water. The recovery yield of Sr was higher than 90% and that of Rb + REEs was nearly 100%. About 1 vol% of each Rb + REEs solution was used to measure Rb with thermal ionization mass spectrometry (TIMS), and the rest of the sample solution was used for Sm-Nd analysis. Second, the REEs was separated from most of matrix elements and Rb from the Rb + REEs solution by passing through a small (7 cm long × 6 mm *i.d.*) ion-exchange column filled with approximately 2 mL AG50W × 12 resin following the method reported by Pin and Zalduegui (1997). Finally, Nd was separated from Sm using LN resin (HDEHP-based, 100–150 mesh, 1.7 mL) as described by Li et al. (2007). The REE fraction was dried down, then dissolved with 0.2 mL of 0.2 M HCl and loaded onto the LN resin column. After rinsing four times with 0.25 mL of 0.2 M HCl, the column was washed with 5.5 mL of 0.25 M HCl. Neodymium was stripped with 6 mL of 0.25 M HCl, and then Sm was stripped with 6 mL of 0.5 M HCl. The total recovery yields of Nd and Sm were about 40% and 90%, respectively. The total procedural blanks ($N$ = 7), including contributions of the tracers and mass spectrometer, were Rb < 5 pg, Sr < 3 pg, Sm < 5 pg and Nd < 10 pg.

Rb and Sm isotopes were measured with the Finnigan-MAT 262 multicollector mass spectrometer at the Institute of Geology and Geophysics, CAS. Sr and Nd isotope ratios were measured with the Thermo-Finnigan Triton TIMS at the Tianjin Institute of Geology and Mineral Resource following the method described by Li et al. (2005, 2007). Strontium was dissolved in a purified $TaF_5$ + $H_3PO_4$ solution and then loaded on a single tungsten filament. Strontium isotopic compositions were calibrated to $^{86}Sr/^{88}Sr$ = 0.1194. The average value of $^{87}Sr/^{86}Sr$ measured for NBS 987 ($N$ = 9, 100–200 ng Sr) was 0.710225 ± 0.000017 (2σ). The measured $^{87}Sr/^{86}Sr$ ratios were normalized to $^{87}Sr/^{86}Sr$ = 0.710250 for NBS 987 (Nyquist et al. 1994). Neodymium was measured as $NdO^+$ on W single-filaments with Silica-gel + $H_3PO_4$ as the ionization enhancer. The average ratios of $^{17}O/^{16}O$ and $^{18}O/^{16}O$ were 0.0003928 and 0.0021297, respectively. Mass-dependent fractionation of Nd was corrected using $^{146}Nd/^{144}Nd$ = 0.72414. The

Table 1. Rb and Sr isotopic compositions of GRV 99027.

| Fraction | Mass[d] (mg) | Rb (ppm) | Sr (ppm) | $^{87}Rb/^{86}Sr$[a] | $^{87}Sr/^{86}Sr$[b] |
|---|---|---|---|---|---|
| Wr1 | 1.43 | 0.31 | 6.38 | 0.1405 ± 14 | 0.711028 ± 27 |
| Wr2-R | 3.60 | 0.66 | 9.92 | 0.1933 ± 19 | 0.710839 ± 16 |
| Wr2-L | 0.20 | 0.56 | 13.7 | 0.1193 ± 26 | 0.711149 ± 24 |
| Wr2-av | | 0.66 | 10.1 | 0.1894 | 0.710856 |
| Fg-R | 6.04 | 0.93 | 11.8 | 0.2287 ± 23 | 0.711006 ± 14 |
| Fg-L | 0.62 | 0.29 | 15.5 | 0.0542 ± 8 | 0.711045 ± 15 |
| Fg-av | | 0.87 | 12.2 | 0.2125 | 0.711009 |
| Ol-1-R | 3.93 | 0.66 | 6.94 | 0.2762 ± 28 | 0.711047 ± 11 |
| Ol-2-R | 2.60 | 0.31 | 3.39 | 0.2630 ± 26 | 0.711015 ± 24 |
| Fe-Px-R | 1.60 | 0.44 | 5.04 | 0.2507 ± 25 | 0.710992 ± 16 |
| Mg-Px-R | 1.54 | 0.35 | 4.56 | 0.2249 ± 22 | 0.710923 ± 17 |
| Pl-R | 2.31 | 2.78 | 83.0 | 0.0962 ± 10 | 0.710603 ± 6 |
| Pl-rich-R | 9.78 | 1.10 | 21.8 | 0.1455 ± 15 | 0.710704 ± 8 |
| Rej-R | 10.37 | 1.16 | 16.3 | 0.2056 ± 21 | 0.710828 ± 7 |
| ΣMin-L | 2.30 | 0.23 | 9.41 | 0.0716 ± 7 | 0.711044 ± 15 |
| NBS 987 ($N$ = 9, 100–200 ng Sr)[c] | | | | | 0.710225 ± 17 |

Wr = whole rock; Fg = fine-grained fraction; Ol = olivine; Fe-Px = Fe-rich pyroxene; Mg-Px = Mg-rich pyroxene; L = leachate; R = residue; av = average, calculated from the residue and corresponding leachate; Rej = impure minerals; Σ Min-L = combined mineral acid leachates.

[a]Uncertainties correspond to last digits and include a minimum uncertainty of 1% plus 50% of the blank correction for Rb and Sr added quadratically.

[b]Normalized to $^{86}Sr/^{88}Sr = 0.1194$ and adjusted to $^{87}Sr/^{86}Sr = 0.710250$ of NBS 987 Sr standard (Nyquist et al. 1994). Uncertainties refer to last digits and are $2\sigma_m$ calculated from the measured isotopic ratios. $2\sigma_m = [\Sigma(m_i - x)^2/(n(n-1))]^{1/2}$ for $n$ ratio measurements $m_i$ with mean value $x$.

[c]Uncertainties refer to last digits and represent $2\sigma_p$ error limits. $2\sigma_p = [\Sigma(M_j - x)^2/(N-1)]^{1/2}$ for $N$ ratio measurements $M_i$ with mean value $x$. Isochrons are calculated using either $2\sigma_p$ (standard runs) or $2\sigma_m$ (measured isotopic ratios), whichever is larger.

[d]Except for the whole rock fraction (Wr1), the weights of other fractions were after the leaching processing.

average ratio of $^{143}Nd/^{144}Nd$ measured for the standard Jndi-1 ($N$ = 14) was 0.511309 ± 14 (2σ). Results of Sr and Nd standard runs were also compiled in Tables 1 and 2, respectively. The Nd isotopic analysis of olivine was abandoned, due to the very low abundance of Nd in olivine (Lin et al. 2005) and the small amount of the sample available in this work.

## RESULTS

### Rb-Sr System

The Rb and Sr concentrations of each sample are listed in Table 1. The Sr concentration of the fine-grained fraction (labeled Fg-av, calculated from the results of the leached sample and the leachate) is higher than that of the whole rock (labeled Wr2-av, calculated from the results of the leached whole rock and the leachate) (12.2 ppm versus 10.1 ppm), suggestive of more Sr-rich components (such as phosphates, plagioclase) in the fine-grained sample. Both the whole rock and the fine-grained fraction are slightly higher than the solution inductively coupled plasma–mass spectrometry (ICP-MS) analyses (9.5 ppm and 7.5 ppm, respectively) (Lin et al. 2008b). The two bulk samples (the unleached Wr1 and the calculated Wr2-av) have different concentrations of Rb (0.31 ppm versus 0.66 ppm) and Sr (6.38 ppm versus 10.1 ppm) and Rb/Sr ratios (0.049 versus 0.065), probably due to inhomogeneity of the small samples (1.43 and 3.60 mg, respectively). The plagioclase fraction has a lower Sr concentration (83 ppm) than the in situ analysis (136 ppm) by SIMS (Lin et al. 2005), probably due to heterogeneity among different grains of this mineral in the both textural regions. The Rb and Sr concentrations of the Ol-1-R fraction are higher than those of pyroxenes, which could be attributed to the common occurrence of magmatic inclusions that contain abundant feldspathic mesostasis in the olivine from GRV 99027 (Lin et al. 2005).

Figure 2 shows Rb-Sr data for GRV 99027. The analyses of Pl-R, Mg-Px-R, Fe-Px-R and two olivine samples (Ol-1-R and Ol-2-R) define a Rb-Sr isochron age of 177 ± 5 (2σ) Ma (MSWD = 0.24) with an initial $^{87}Sr/^{86}Sr$ ratio of 0.710364 ± 11 (2σ), using $\lambda(^{87}Rb) = 1.402 \times 10^{-11}$ yr$^{-1}$. Inclusion of the Pl-rich-R, Wr2-R and impure minerals (Rej-R) fractions modifies the isochron age slightly to 180 ± 20 Ma (MSWD = 14, 2σ) with an initial $^{87}Sr/^{86}Sr = 0.710346 \pm 58$ (2σ). Although the two isochron ages are the same within the analytical uncertainties, the age of 177 ± 5 (2σ) Ma is preferred, because this isochron is defined with the pure

Table 2. Sm and Nd isotopic compositions of GRV 99027.

| Fraction | Mass[a] (mg) | Sm (ppm) | Nd (ppm) | Nd[f] (ng) | $^{147}Sm/^{144}Nd$[b] | $^{143}Nd/^{144}Nd$[c] |
|---|---|---|---|---|---|---|
| Wr1 | 6.83 | 0.28 | 0.52 | 1.23 | 0.3261 ± 16 | 0.512620 ± 18 |
| Wr2-R | 7.85 | 0.06 | 0.09 | 0.26 | 0.4223 ± 71 | 0.512796 ± 85 |
| Wr2-L | 0.71 | 2.98 | 5.23 | 1.30 | 0.3447 ± 17 | 0.512554 ± 11 |
| Wr2-av | | 0.31 | 0.52 | | 0.4159 | 0.512776 |
| Fg-R | 6.04 | 0.07 | 0.09 | 0.19 | 0.4699 ± 101 | 0.513565 ± 67[d] |
| Fg-L | 0.62 | 6.23 | 10.8 | 2.34 | 0.3490 ± 17 | 0.512526 ± 14 |
| Fg-av | | 0.64 | 1.09 | | 0.4587 | 0.513468 |
| ∑Min-L | 2.30 | 5.94 | 10.1 | 8.14 | 0.3555 ± 18 | 0.512501 ± 15 |
| Rej-R | 10.37 | 0.08 | 0.13 | 0.34 | 0.3805 ± 71 | 0.512546 ± 23 |
| Fe-Px-R | 16.80 | 0.06 | 0.09 | 0.35 | 0.4330 ± 92 | 0.513283 ± 19[d] |
| Mg-Px-R | 15.56 | 0.03 | 0.07 | 0.25 | 0.2856 ± 102 | 0.512139 ± 24[d] |
| Pl-R | 3.53 | 0.15 | 0.26 | 0.32 | 0.3423 ± 25 | |
| Pl-rich-R | 9.78 | | | | | |
| Jndi-1 ($N$ = 14)[g] | | | | | | 0.511309 ± 14[e] |
| Jndi-1 ($N$ = 5)[h] | | | | | | 0.511322 ± 15[e] |

Abbreviations are the same as in Table 1.
All $NdO^+$ runs at above 0.1 v of $^{144}Nd$ beam intensities except Fg-R, Fe-Px-R and Mg-Px-R ($^{144}Nd$ < 80 mv).
[a]Except for the whole rock fraction (Wr1), the weights of other fractions were after the leaching processing.
[b]Uncertainties correspond to last digits and include a minimum uncertainty of 0.5% plus 50% of the blank correction for Sm and Nd added quadratically.
[c]Normalized to $^{146}Nd/^{144}Nd = 0.72414$. Uncertainties correspond to last digits and are $2\sigma_m$ calculated from the measured isotopic ratios. $2\sigma_m = [\Sigma(m_i - x)^2/(n(n-1))]^{1/2}$ for $n$ ratio measurements $m_i$ with mean value $x$.
[d]The value of $^{143}Nd/^{144}Nd$ may be questionable, due to low $^{144}Nd$ beam intensities (50–80 mv).
[e]Uncertainties refer to last digits and represent $2\sigma_p$ error limits. $2\sigma_p = [\Sigma(M_j - x)^2/(N-1)]^{1/2}$ for $N$ ratio measurements $M_i$ with mean value $x$. Isochrons are calculated using either $2\sigma_p$ (standard runs) or $2\sigma_m$ (measured isotopic ratios), whichever is larger.
[f]Total recovery of Nd.
[g]Run as $NdO^+$.
[h]Run as Nd.

mineral separates and the analyses of impure fractions (Pl-rich-R and Rej-R) show more scatter.

The three leachate fractions plot far above the 177 Ma isochron, indicating that GRV 99027 contains leachable components that are not in isotopic equilibrium with the silicate phases. These components are also detectable in the unleached whole rock fraction (Wr1), which plots between the leachate fractions and the leached samples. This suggests that the Rb-Sr system of GRV 99027 has been disturbed. In addition, the leached fine-grained fraction (Fg-R) also plots above and to the left of the 177 Ma isochron (upward by +0.9 ε-unit, $\varepsilon_{Sr} = [(^{87}Sr/^{86}Sr)_{measured}/(^{87}Sr/^{86}Sr)_{isochron} - 1] \times 10{,}000$), suggesting that the fine-grained fraction probably contains unleachable components with higher $^{87}Sr/^{86}Sr$.

## Sm-Nd System

All fractions have low abundances of Nd and Sm, especially the mineral fractions (the recovered Nd is less than 0.4 ng, Table 2), hence there are relatively large analytical uncertainties. In addition, we could not obtain Nd isotope analyses of the Pl-R and Pl-rich-R fractions due to the small amounts of the samples. The Nd isotopic ratios of the leached whole rock (Wr2-R) have large errors, while those of the leached fine-grained (Fg-R), Fe-Px-R, and Mg-Px-R fractions may be questionable, because of very low signal intensities of $^{144}Nd$ (50–80 mv).

The concentrations of Sm and Nd for GRV 99027 are listed in Table 2 and plotted in Fig. 3 in comparison with the data from our earlier studies (Lin et al. 2005, 2008b). The Sm and Nd concentrations of the calculated fine-grained fraction (Fg-av) are twice as high as those of the whole rock (Wr1, Wr2-av), and both the Sm and Nd concentrations of these fractions are nearly the same as those determined by solution ICP-MS (Lin et al. 2008b). Our analyses confirm higher Sm and Nd concentrations of the fine-grained sample compared with the bulk meteorite, suggestive of more REE-rich minerals (e.g., phosphates) in this fraction. The leached whole rock (Wr2-R) and fine-grained (Fg-R) fractions have lower Sm and Nd concentrations with slightly higher Sm/Nd ratios than the ICP-MS data, indicating that most of Sm and Nd were leachable and the Sm/Nd ratios of the residues were mainly controlled by LREE-depleted minerals such as pyroxenes. In situ SIMS analysis revealed large ranges of REE concentrations of pigeonite and augite in GRV 99027 (Lin et al. 2005), and the Sm and Nd abundances of Fe-Px and Mg-Px fractions are within these ranges. The plagioclase (Pl-R) fraction may contain heavy rare earth element-enriched

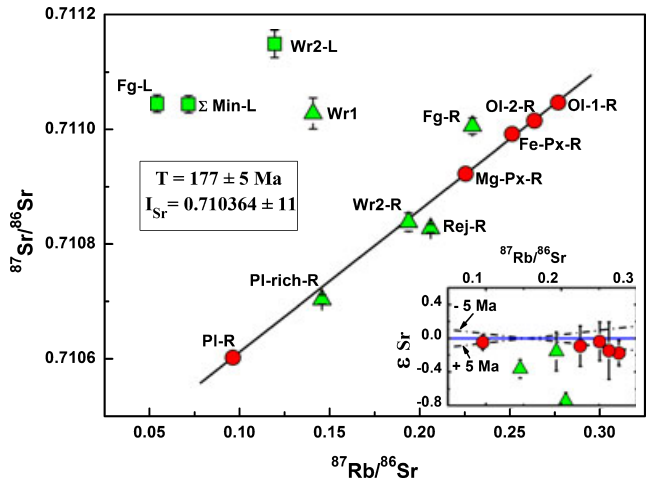


Fig. 2. Rb-Sr isochron for GRV 99027. Regression of the isochron and age calculation were carried out on the circles only using ISOPLOT software (Ludwig 2005). The inset depicts the deviation ($\varepsilon_{Sr}$) of the individual points from the 177 Ma isochron (solid line). The dashed lines represent ±5 Ma corresponding to the 177 Ma isochron. $\varepsilon_{Sr} = [(^{87}Sr/^{86}Sr)_{measured}/(^{87}Sr/^{86}Sr)_{isochron} - 1] \times 10{,}000$. Abbreviations are the same as in Table 1.

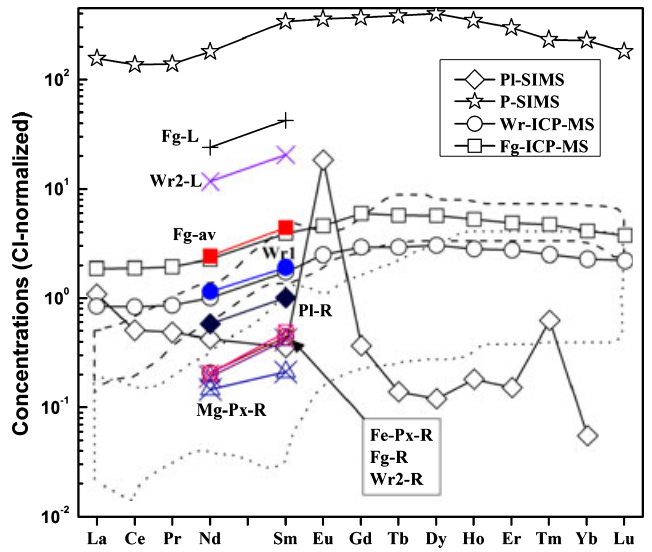


Fig. 3. CI-normalized Sm and Nd abundances of the mineral fractions of GRV 99027, compared with REE patterns of the bulk samples determined by ICP-MS (Lin et al. 2008b) and the individual minerals determined in situ by SIMS (Lin et al. 2005). Abbreviations are the same as in Table 1, and the compositional ranges of pigeonite and augite are outlined with dotted and dashed lines, respectively.

components (likely phosphates) that increase the Sm/Nd ratio relative to the SIMS in situ analysis. The leachate fractions have nearly the same $(Sm/Nd)_{CI}$ ratios (1.8 × CI) as the SIMS analysis of phosphates from GRV 99027 (1.9 × CI) (Lin et al. 2005).

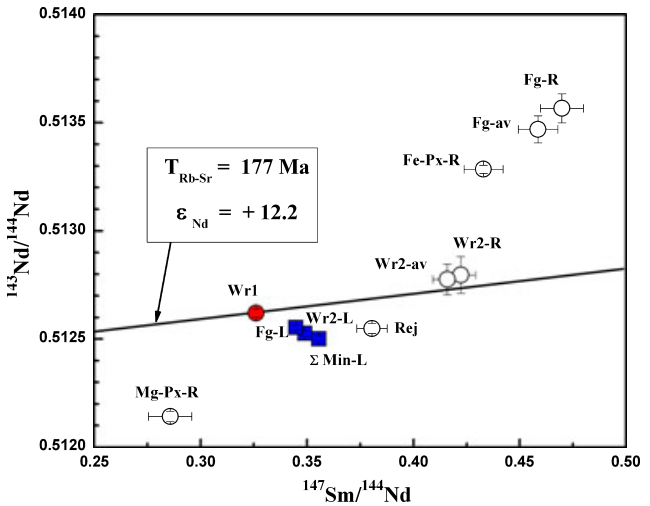


Fig. 4. Sm-Nd isotopic data for GRV 99027. The analyses are scattered and do not define a simple isochron. The color-filled analyses have Nd > 1 ng. A reference line of 177 Ma across the analysis of Wr1 is also shown. Abbreviations are the same as in Table 1.

The Sm-Nd isotopic data of GRV 99027, plotted in Fig. 4, do not establish a reliable isochron. Only nine sample fractions were determined for Nd isotopic compositions with three analyses questionable due to the very small amounts of Nd (0.19–0.35 ng; Table 2). Beside the leachates, only the whole rock sample Wr1 has a high amount of Nd (1.23 ng), hence the analysis of Sm-Nd of Wr1 is robust. The $\varepsilon^{143}Nd$ of GRV 99027 is estimated to be approximately +12.2 from the Sm-Nd isotopic data of Wr1 assuming the same age of 177 Ma determined from the Rb-Sr isochron.

All leachates plot below the reference line of 177 Ma. The leached impure mineral fraction (Rej-R) also deviates from the reference line. The deviation is due to the low amount of Nd of Rej-R (0.34 ng), which is a challenge even for Triton, the most updated type of TIMS.

## DISCUSSION

### Disturbance of Rb-Sr Isotopic System of GRV 99027

The $^{87}Sr/^{86}Sr$ ratios of the leachate fractions of GRV 99027 are significantly higher than the modern seawater value of approximately 0.709, and therefore cannot be attributed to terrestrial weathering. In fact, GRV 99027 was found on blue ice in Antarctic, and shows few weathering effects (Lin et al. 2005). The enhancement of $^{87}Sr/^{86}Sr$ ratios in the leachate fractions has also been reported in other lherzolitic shergottites (ALHA77005) (Borg et al. 2002) and has been explained as the result of heavy shock or contamination by secondary alteration products, which disturbed the Rb-Sr system. The leachate fractions of GRV 99027 have the highest $^{87}Sr/^{86}Sr$ ratios

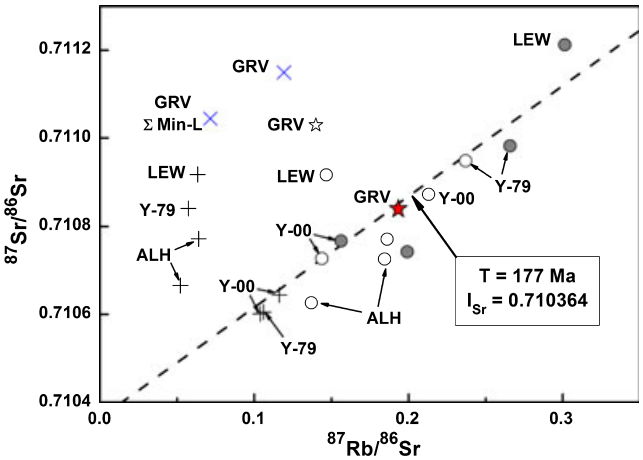


Fig. 5. Rb-Sr isotopic data of lherzolitic shergottites showing leached whole rocks (filled star or circle), unleached whole rocks (open star or circle), the leachates of GRV 99027 (×), the leachates of other meteorites (+). The reference Rb-Sr isochron age of 177 Ma (dashed line) with an initial $^{87}Sr/^{86}Sr$ = 0.710364 is also plotted. GRV = GRV 99027; ALH = ALHA77005; LEW = LEW 88516; Y-79 = Y-793605; Y-00 = Y-000097. Literature data are from Morikawa et al. (2001), Borg et al. (2002), and Misawa et al. (2008).

of intermediate subgroup lherzolitic shergottites (Fig. 5), consistent with the strong shock metamorphism and extensive postshock thermal metamorphism experienced by this meteorite. All lherzolitic shergottites were heavily shocked, as indicated by presence of melt veins, mosaic extinction of olivine and pyroxene, and transformation of plagioclase to glass (Nyquist et al. 2001; Fritz et al. 2005; Lin et al. 2005; Wang and Chen 2006). However, they experienced different degrees of thermal metamorphism after the major impact event, and GRV 99027 appears to be the most intensely modified (Lin et al. 2005). The strong shock metamorphism and postshock thermal metamorphism may cause radiogenic daughter isotopes to diffuse to grain boundaries, where they are preferentially leachable with weak acid (Gaffney et al. 2007). In addition, enhancement of the $^{87}Sr/^{86}Sr$ ratios may be partially attributed to contamination with components with high $^{87}Sr/^{86}Sr$ ratios. For instance, Martian crust, with high $^{87}Sr/^{86}Sr$ ratios (Wadhwa 2001), can contaminate the meteorites through alteration as suggested by Borg et al. (2002). However, evidence for such alteration in GRV 99027 is not extensive.

## Genetic Relationship Among Lherzolitic Shergottites

Our previous study of GRV 99027 demonstrated that it has the most similar petrography and mineral chemistry of ALHA77005 (Lin et al. 2005), probably paired with the latter. However, the initial $^{87}Sr/^{86}Sr$ ratio of GRV 99027 (0.710364 ± 11) determined here is clearly distinguishable from that of ALHA77005 (0.71026 ± 4) (Borg et al. 2002), excluding this possibility. Hence, the Rb-Sr mineral isochron age of 177 ± 5 Ma of GRV 99027 confirms the same age of approximately 180 Ma for all meteorites of the intermediate subgroup. Up to date, only five of 10 meteorites of this subgroup were dated with Rb-Sr and/or Sm-Nd mineral isochron methods, and four of them have the similar ages within the analytical uncertainties, including ALHA77005 (185 ± 11 Ma), LEW 88516 (183 ± 10 Ma) (Borg et al. 2002), Y-793605 (173 ± 14 Ma) (Morikawa et al. 2001), and Y-984028 (170 ± 9 Ma) (Shih et al. 2011). A younger Rb-Sr mineral isochron age (147 ± 28 Ma) was reported for Y-000097 (Misawa et al. 2008), but it is indistinguishable from the others considering its large analytical uncertainty. The same age of approximately 180 Ma for all meteorites of the intermediate subgroup is unlikely to be a statistical bias, because the number of samples has been updated to five even Y-000097 is not counted.

The similar radiometric mineral isochron ages of lherzolitic shergottites are consistent with their delivery from the same or several similar igneous units on the Mars. In addition, the latter scenario that these meteorites have individual but similar source regions was supported by the small but distinguishable differences in the initial $^{87}Sr/^{86}Sr$ ratios between ALHA77005 (0.71026 ± 4) and LEW 88516 (0.71052 ± 4) (Borg et al. 2002). However, this small gap in the initial $^{87}Sr/^{86}Sr$ ratios has been filled with the analyses of Y-793605 (0.71042 ± 7) (Morikawa et al. 2001), Y-984028 (0.710389 ± 29) (Shih et al. 2011), and GRV 99027 (0.710364 ± 11) reported here. Alternatively, all meteorites of the intermediate subgroup may originate from the same igneous unit on Mars. The continuous initial $^{87}Sr/^{86}Sr$ ratios of lherzolitic shergottites can be attributed to various degrees of assimilation of the evolved Martian crust with higher $I_{Sr}$ (Wadhwa 2001) by the parent magma. This possibility is also consistent with their similarities in petrography, mineral chemistry, trace elements, and ejection ages between GRV 99027 (Hsu et al. 2004; Lin et al. 2005; Kong et al. 2007) and other lherzolitic shergottites. The new data of GRV 99027 reinforce the scenario that lherzolitic shergottites of the intermediate subgroup originated from the same source region.

Because of larger uncertainties in the Sm-Nd results, these data provide few constraints on the genetic relationship of GRV 99027 with other members of this subgroup. The estimated $\varepsilon^{143}Nd$ value of GRV 99027 (+12.2) is distinct from those of LEW 88516 (8.2 ± 0.6) and Y-793605 (9.7 ± 0.2), but close to ALHA77005 (11.1 ± 0.2) and Y-000097 (11.7 ± 0.2) (Borg et al. 2002; Misawa et al. 2006, 2008).

## CONCLUSIONS

The Rb-Sr and Sm-Nd isotopic systems of the lherzolitic shergottite GRV 99027 were studied. The leached pure mineral fractions yield a Rb-Sr isochron with an age of 177 ± 5 (2σ) Ma and an initial $^{87}Sr/^{86}Sr$ ratio of 0.710364 ± 11 (2σ). The analyses of Nd isotopic compositions have large uncertainties due to the very small amounts of Nd, and it is not possible to establish a Sm-Nd isochron for GRV 99027. The $\varepsilon^{143}Nd$ value of GRV 99027 is estimated approximately +12.2 from the whole rock sample assuming the Rb-Sr isochron age of 177 Ma.

The leachates of GRV 99027 have high $^{87}Sr/^{86}Sr$ ratios, plotting significantly above the Rb-Sr mineral isochron. This suggests contamination by components with high $^{87}Sr/^{86}Sr$ ratios and/or significant disturbance by intense impact events consistent with the strong shock effects and extensive postshock thermal metamorphism of GRV 99027 (Lin et al. 2005).

The $I_{Sr}$ of GRV 99027 is distinguishable from other lherzolitic shergottites, confirming the previous conclusion that this meteorite is not paired with the latter. The Rb-Sr mineral isochron age of GRV 99027 makes the same age of approximately 180 Ma a robust statistical result for the lherzolitic shergottites of the intermediate subgroup. Furthermore, the $I_{Sr}$ of GRV 99027 (0.710364 ± 11) and those of Y-793605 (0.71042 ± 7) (Morikawa et al. 2001) and Y-984028 (0.710389 ± 29) (Shih et al. 2011) fill the small gap between ALHA77005 (0.71026 ± 4) and LEW 88516 (0.71052 ± 4) (Borg et al. 2002). The continuous $I_{Sr}$ values of these meteorites can be explained by various degrees of assimilation of the evolved Martian crust with higher $I_{Sr}$ (Wadhwa 2001) by the parent magma.

*Acknowledgments*—The manuscript has been significantly improved by the constructive reviews by S. Symes and two other anonymous reviewers, and the associate editor, C. Floss. The sample of GRV 99027 was provided by the Polar Research Institute of China, and this study was supported by the Knowledge Innovation Program of Chinese Academy of Sciences (KZCX2-YW-Q08, kzcx2-yw-110).

*Editorial Handling*—Dr. Christine Floss

## REFERENCES

Anand M., James S., Greenwood R. C., Johnson D., Franchi I. A., and Grady M. M. 2008. Mineralogy and geochemistry of shergottite RBT 04262 (abstract #2173). 39th Lunar and Planetary Science Conference. CD-ROM.

Borg L. E., Nyquist L. E., Wiesmann H., and Reese Y. 2002. Constraints on the petrogenesis of Martian meteorites from the Rb-Sr and Sm-Nd isotopic systematics of the lherzolitic shergottites ALH 77005 and LEW 88516. *Geochimica et Cosmochimica Acta* 66:2037–2053.

Bouvier A., Blichert-Toft J., Vervoort J., and Albarède F. 2005a. The age of Zagami and other shergottites. *Meteoritics & Planetary Science* 40:5038.

Bouvier A., Blichert-Toft J., Vervoort J. D., and Albarède F. 2005b. The age of SNC meteorites and the antiquity of the Martian surface. *Earth and Planetary Science Letters* 240:221–233.

Bouvier A., Blichert-Toft J., Vervoort J. D., Gillet P., and Albarède F. 2008. The case for old basaltic shergottites. *Earth and Planetary Science Letters* 266:105–124.

Bouvier A., Blichert-Toft J., and Albarède F. 2009. Martian meteorite chronology and the evolution of the interior of Mars. *Earth and Planetary Science Letters* 280:285–295.

Bridges J. C. and Warren P. H. 2006. The SNC meteorites: Basaltic igneous processes on Mars. *Journal of Geological Society* 163:229–251.

Fritz J., Artemieva N., and Greshake A. 2005. Ejection of Martian meteorites. *Meteoritics & Planetary Science* 40:1393–1411.

Gaffney A. M., Borg L. E., and Asmerom Y. 2007. Disturbance of Sm-Nd, Rb-Sr and U-Pb isochrons during shock and thermal metamorphism—An experimental approach (abstract #1424). 38th Lunar and Planetary Science Conference. CD-ROM.

Goodrich C. A. 2002. Olivine-phyric Martian basalts: A new type of shergottite. *Meteoritics & Planetary Science* 37:31–34.

Herd C. D. K., Simonetti A., and Peterson N. D. 2007. In situ U-Pb geochronology of Martian baddeleyite by laser ablation MC-ICP-MS (abstract #1664). 38th Lunar and Planetary Science Conference. CD-ROM.

Hsu W., Guan Y., Wang H., Leshin L. A., Wang R., Zhang W., Chen X., Zhang F., and Lin C. 2004. The lherzolitic shergottite Grove Mountains 99027: Rare earth element geochemistry. *Meteoritics & Planetary Science* 39:701–709.

Jagoutz E. 1989. Sr and Nd isotopic systematics in ALHA77005: Age of shock metamorphism in shergottites and magmatic differentiation on Mars. *Geochimica et Cosmochimica Acta* 53:2429–2441.

Kong P., Fabel D., Brown R., and Freeman S. 2007. Cosmic-ray exposure age of Martian meteorite GRV 99027. Science in China. Series D: *Earth Sciences* 50:1521–1524.

Li C., Chen F., and Li X. 2007. Precise isotopic measurements of sub-nanogram Nd of standard reference material by thermal ionization mass spectrometry using the $NdO^+$ technique. *International Journal of Mass Spectrometry* 266:34–41.

Li Q., Chen F., Wang X., Li X., and Li C. 2005. Ultra-low procedural blank and the single-grain mica Rb-Sr isochron dating. *Chinese Science Bulletin* 50:2861–2865.

Lin Y., Ouyan Z., Wang D., Miao B., Liu X., Kimura M., and Jun Y. 2002. Grove Mountains (GRV) 99027: A new Martian lherzolite. *Meteoritics & Planetary Science* 37:A87.

Lin Y., Wang D., Miao B., Ouyang Z., Liu X., and Ju Y. 2003. Grove Mountains (GRV) 99027: A new Martian meteorite. *Chinese Science Bulletin* 48:1771–1774.

Lin Y., Guan Y., Wang D., Kimura M., and Leshin L. A. 2005. Petrogenesis of the new lherzolitic shergottite Grove Mountains 99027: Constraints of petrography, mineral chemistry, and rare earth elements. *Meteoritics & Planetary Science* 40:1599–1619.

Lin Y., Liu T., Shen W., Xu L., and Miao M. 2008a. Grove Mountains (GRV) 020090: A highly fractionated lherzolitic shergottite (abstract). *Meteoritics & Planetary Science* 43:A86.

Lin Y., Qi L., Wang G., and Xu L. 2008b. Bulk chemical composition of lherzolitic shergottite Grove Mountains (GRV) 99027—Constraints on the mantle of Mars. *Meteoritics & Planetary Science* 43:1179–1187.

Ludwig K. R. 2005. *Users manual for isoplot/ex: A geochronological toolkit for Microsoft Excel*. BGC Special Publication 53. Berkeley, California: Berkeley Geochronology Center.

McSween H. Y. Jr. 1994. What we have learned about Mars from SNC meteorites. *Meteoritics* 29:757–779.

Miao B., Ouyang Z., Wang D., Ju Y., Wang G., and Lin Y. 2004. A new Martian meteorite from Antarctica: Grove Mountains (GRV) 020090. *Acta Geologica Sinica* 78:1034–1041.

Misawa K. and Yamaguchi A. 2007. U-Pb ages of NWA 856 baddeleyite (abstract #5228). *Meteoritics & Planetary Science* 42:A108.

Misawa K., Yamazaki F., Ihira N., and Nakamura N. 2000. Separation of rare earth elements and strontium from chondritic meteorites by miniaturized extraction chromatography for elemental and isotopic analyses. *Geochemical Journal* 34:11–22.

Misawa K., Yamada K., Nakamura N., Morikawa N., Kondorosi G., Yamashita K., and Premo W. R. 2006. Sm-Nd isotopic systematics of lherzolitic shergottite Yamato-793605. *Antarctic Meteorite Research* 19:45–57.

Misawa K., Park J., Shih C. Y., Reese Y., Bogard D. D., and Nyquist L. E. 2008. Rb-Sr, Sm-Nd, and Ar-Ar isotopic systematics of lherzolitic shergottite Yamato 000097. *Polar Science* 2:163–174.

Morikawa N., Misawa K., Kondorosi G., Premo W. R., Tatsumoto M., and Nakamura N. 2001. Rb-Sr isotopic systematics of lherzolitic shergottite Yamato-793605. *Antarctic Meteorite Research* 14:47–60.

Nyquist L. E., Bansal B., Wiesmann H., and Shih C.-Y. 1994. Neodymium, strontium and chromium isotopic studies of the LEW 86010 and Angra dos Reis meteorites and the chronology of the angrite parent body. *Meteoritics* 29:872–885.

Nyquist L. E., Bogard D. D., Shih C. Y., Greshake A., Stöffler D., and Eugster O. 2001. Ages and geologic histories of Martian meteorites. *Space Science Reviews* 96:105–164.

Ozawa S., Ireland T. R., El Goresy A., and Ohtani E. 2009. U-Pb dating of baddeleyites in two shergottites and a chassignite after careful petrographic characterization. AGU Fall Meeting Abstracts, #MR12A-05.

Pin C. and Zalduegui J. F. 1997. Sequential separation of light rare-earth elements, thorium and uranium by miniaturized extraction chromatography: Application to isotopic analyses of silicate rocks. *Analytica Chimica Acta* 339: 79–89.

Shih C. Y., Nyquist L. E., Bogard D. D., McKay G. A., Wooden J. L., Bansal B. M., and Wiesmann H. 1982. Chronology and petrogenesis of young achondrites, Shergotty, Zagami, and ALHA77005: Late magmatism on a geologically active planet. *Geochimica et Cosmochimica Acta* 46:2323–2344.

Shih C. Y., Nyquist L. E., Reese Y., and Misawa K. 2011. Sm-Nd and Rb-Sr studies of lherzolitic shergottite Yamato 984028. *Polar Science* 4:515–529.

Symes S. J. K., Borg L. E., Shearer C. K., and Irving A. J. 2008. The age of the Martian meteorite Northwest Africa 1195 and the differentiation history of the shergottites. *Geochimica et Cosmochimica Acta* 72:1696–1710.

Usui T., Sanborn M. E., Wadhwa M., and McSween H. Y. 2008. Petrogenesis of geochemically enriched lherzolitic shergottites RBT 04261 and RBT 04262 (abstract). *Meteoritics & Planetary Science* 43:A159.

Wadhwa M. 2001. Redox state of Mars' upper mantle and crust from Eu anomalies in shergottite pyroxenes. *Science* 291:1527–1530.

Wang D. and Chen M. 2006. Shock-induced melting, recrystallization, and exsolution in plagioclase from the Martian lherzolitic shergottite GRV 99027. *Meteoritics & Planetary Science* 41:519–527.